New Approach to Definition of Potential of the Electric Field Created by Set Distribution in Space of Electric Charges

E.G.Ismibayli, I.J.Islamov, Y.G.Gaziyev

***Abstract*— We study the dependence of the rate of convergence of the relaxation process on the value of ω. We compare the rate of convergence of methods for the upper and lower relaxation. We calculate the dependence of the potentials difference on the distance between two linear charges. The obtained numerical results are compared with the recognized analytical solution of this problem. The dependence of the rate of convergence of the relaxation techniques and the accuracy of the numerical solution on the step of grid is investigated here. Algorithms, allowing visualization of the distribution process of the electric field strength have been created.**

***Index Terms*— potential, electric field, Laplace equation, Poisson's equation, relaxation method**

I. INTRODUCTION

Currently, the capacity to find the electric field at the location of the unknown source of charges, but in given electric potential at the boundaries of the field generated by the fixed wire system, placed in a vacuum and connected to the batteries, is an urgent task of electrostatics. It is possible to measure the potential of each of the conductor, but setting the distribution of electrical charges on the conductors, depending on their shape, is very difficult. On the other hand, the received more accurate theoretical results enable to design and construct the above-mentioned electrostatic systems optimally. For this purpose, in this paper we propose a new approach to determining the potential of the electric field produced by a given distribution of electric charges in the space, which makes it possible to more accurately determine the distribution of the electric field.

It is known [1] that the direct method of calculation of the electric field potential $\varphi(x, y, z)$ in electrostatic problems is to solve the Laplace equation

$$\Delta\varphi(x, y, z) = \frac{\partial^2\varphi}{\partial x^2} + \frac{\partial^2\varphi}{\partial y^2} + \frac{\partial^2\varphi}{\partial z^2} = 0, \quad (1)$$

and Poisson's equation

$$\Delta\varphi(x, y, z) = \frac{\partial^2\varphi}{\partial x^2} + \frac{\partial^2\varphi}{\partial y^2} + \frac{\partial^2\varphi}{\partial z^2} = -\rho(x, y, z). \quad (2)$$

Equations (1) and (2) belong to a class of partial differential equations of elliptic type. It should be noted that in some cases the required spatial field is close to the rotation of the field, especially in the most important for the practice – the area near the high-voltage current-carrying conductors, having the greatest practical importance. Therefore, for simplicity of calculations we shall further consider the special case of elliptic equations for the field $\varphi(x, y)$, which depends on two spatial variables. It is obvious that to fully address the problem of the equation (1), (2) it must be supplemented with the boundary conditions. There are three types of boundary conditions:

1) Dirichlet boundary conditions (values of φ are given on a closed curve in the plane (x, y), and possibly some additional curves situated inside the field); 2) Neumann boundary conditions (normal derivative of the potential φ is defined on the border φ); 3) mixed boundary value problem (linear combination of the potential φ and its normal derivative is defined on the border. Dirichlet boundary conditions are satisfied for the test case.

II. METHODS OF NUMERICAL SOLUTION

We consider the methods of numerical solution of the more general equation (2), assuming that the solution is searched in a single square. As a first step of obtaining the numerical solutions, let us transform the equation (2) into a form convenient for numerical solution. To do this, in the plane (x, y) we define a grid of (N + 1)×(N + 1) nodes, covering the treated area. For simplicity, we choose h grid spacing for each coordinate axis as uniform and equal. Grid nodes will be denoted by a pair of indices (i, j), running from 0 to N. In the chosen notation, the coordinates of the point (i, j) are equal $(x = ih, y = jh)$. Denoting the values of the functions φ and ρ at the nodal points, respectively $\varphi_{ij} = \varphi(x_i, y_j)$, $\rho_{ij} = \rho(x_i, y_j)$, and using a 3-point formula [2-4] for approximation, we obtain the difference approximation of equation (2) of the current-carrying conductors having the greatest practical importance. Therefore, for simplicity of calculations we shall consider the special case of elliptic equations for the field $\varphi(x, y)$, which depends on two spatial variables. It is obvious that to fully address the problem of the equation [2-4], it is necessary to

Manuscript received March 23, 2016
E.G.Ismibayli, Department of "Radio Engineering and telecommunications" of Azerbaijan Technical University, Baku, Azerbaijan
I.J.Islamov, Department of "Radio Engineering and telecommunications" of Azerbaijan Technical University, Baku, Azerbaijan
Y.G.Gaziyev, Department of "Radio Engineering and telecommunications" of Azerbaijan Technical University, Baku, Azerbaijan

supplement it by the boundary conditions. There are three types of boundary conditions:

$$\frac{\varphi_{i+1,j}+\varphi_{i-1,j}-2\varphi_{ij}}{h^2}+\frac{\varphi_{i,j+1}+\varphi_{i,j-1}-2\varphi_{ij}}{h^2}=-\rho_{ij}, \quad (3)$$

here $\varphi_0=\varphi(0),\varphi_N=\varphi(1)$.

Equation (3) gives a system of linear equations for the unknown variables $\varphi(i=1,N-1)$, the matrix of the system of equations is tridiagonal (ie the nonzero elements in the matrix are only the elements located on the main diagonal and the two diagonals, above and below the main diagonal). For a small number of points (for example, N≤100) this system of equations can be solved by direct methods [5-6], or by using the special direct method developed to solve the "tridiagonal" systems [7]. However, in practice, with the numerical solution of elliptic equations, we have to use the girds with a much larger number of nodes, as typical now computer with the processor of Pentium IV/3GHz/512Mb that allows calculating three hours nonlinear problem with 15 million units. It is therefore advisable to consider only iterative methods (for example, relaxation techniques), applied for large sparse matrices.

III. APPLICATION OF RELAXATION METHOD

We rewrite the equation (3), determining it with respect to variable φ_i :

$$\varphi_{ij}=\frac{1}{4}\left[\varphi_{i+1,j}+\varphi_{i-1,j}+\varphi_{i,j+1}+\varphi_{i,j-1}+h^2\rho_{ij}\right]. \quad (4)$$

Despite the fact that the values of $\varphi_{i-1,j},\varphi_{i+1,j},\varphi_{i,j-1},\varphi_{i,j+1}$, included into the right-hand side of (4) are not known, they can be interpreted as a "refinement" values of $\varphi_{i,j}$ through the values at neighboring points. A method for solving the equation (4) (Gauss-Seidel method) is as follows:

1) to select a first approximation for the solution of the equation (4);

2) moving on the grid (for example, left to right), to clarify the solution in accordance with equation (4). Initial approximation can come together ("get relaxed") to the exact solution with multiple repetition of the described process.

In practice, instead of equation (4), it is used a generalized equation, where in each relaxation step $\varphi_{i,j}$ is replaced by a linear combination of its old value and an "improved" by the formula (4)

$$\varphi_{i,j}\to\varphi'_{i,j}=(1-\omega)\varphi_{i,j}+\frac{\omega}{4}(\varphi_{i+1,j}+\varphi_{i-1,j}+\varphi_{i,j+1}+\varphi_{i,j-1}+h^2\rho_{i,j}). \quad (5)$$

To investigate the convergence of this procedure we calculate the change of functional of energy E defined with the following formula

$$E'-E=-\frac{\omega(2-\omega)}{h}\left[\frac{1}{4}(\varphi_{i+1j}+\varphi_{i-1,j}+\varphi_{i,j+1}+\varphi_{i,j-1}-h^2\rho_{i,j})-\varphi_{i,j}\right]^2 \quad (6)$$

From (6) we see that when $\omega\in]0;2[$ energy is increasing and therefore the iterative process will converge to the required minimum value. The existence of foreign energy minima indicates ill-conditioned linear systems. Parameter ω determines the speed of convergence of the iterative process - relaxation rate. When $\omega<1$, it is used the method of "under-relaxation", with $\omega>1$ - a method of "over-relaxation".

The algorithm containing the solution to the boundary value problem can be represented as follows:

1) Setting function $\rho(x,y)$;

2) Setting a function that implements an iterative procedure, here $E-$ the number of points where the values of the function are calculated; $\omega-$ parameter that specifies the method of relaxation; N of Iter-the number of iterations; $\rho(x,y)$ - the function name

$$iteration(N,\omega,N\_Iter,\rho(x,y))=\left|\begin{array}{l} h\leftarrow\frac{1}{N} \\ for\, i,j\in 0...N \\ \left|\begin{array}{l} x\leftarrow ih, jh \\ \rho_{ij}\leftarrow\rho(x,y) \\ \varphi_{i,j}\leftarrow 0 \\ for N\_Inter\in 0...N\_Inter-1, if N\_Inter\neq 0 \\ for\, i,j\in 1...N-1 \\ \varphi_{i,j}\leftarrow(1-\omega)\varphi_{i,j}+\frac{\omega}{4}(\varphi_{i+1,j}+\varphi_{i-1,j}+\varphi_{i,j+1}+\varphi_{i,j-1}+h^2\rho_{ij}) \\ \varphi \end{array}\right. \end{array}\right.$$

3) setting a function, which is an exact solution of the boundary $F(x,y)$;

4) construction of the boundary problem solutions graphs for different numbers of iterations (fig.1)

$$N_i=100, j=0...N_i, y_j=\frac{1}{N_i},$$

$$N=20, k=0...N, z_k=\frac{k}{N}.$$

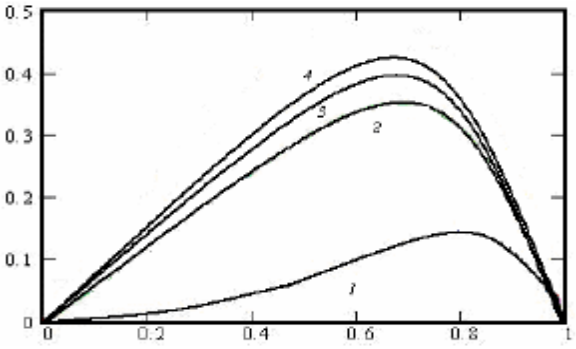

Fig.1. Charts solving boundary value problems for a number of different iterations:
$1-iteration(N,1,150,\rho)_k$; $2-iteration(N,1,50,\rho)_k$;
$3-iteration(N,1,10,\rho)_k$; $4-F(y_i)$.

To demonstrate the convergence of the iterative process, you can plot the energy functional, as a function of the number of iterations. To do this, the algorithm described above must be supplemented by the following algorithm.

5) Specifying a function that returns the value of energy

$$iter\_e(N,\omega,N\_Iter,\rho(x,y)) = \left|\begin{array}{l} h \leftarrow \frac{1}{N} \\ for\, i,j \in 0...N \\ \left|\begin{array}{l} x \leftarrow ih, jh \\ \rho_{i,j} \leftarrow \rho(x,y) \\ \varphi_{i,j} \leftarrow 0 \end{array}\right. \\ for\, k \in 0...N\_Inter \\ \left|\begin{array}{l} for\, i,j \in 0...N-1 \\ \left|\begin{array}{l} \varphi_{i,j} \leftarrow (1-\omega)\varphi_{i,j} + \frac{\omega}{4}(\varphi_{i+1,j} + \varphi_{i-1,j} + \varphi_{i,j+1} + \varphi_{i,j-1} + h^2\rho_{i,j}) \end{array}\right. \\ e \leftarrow 0 \\ for\, i,j \in 1...N \\ \left|\begin{array}{l} e \leftarrow e + \frac{(\varphi_{i,j} - \varphi_{i-1,j})^2}{4h} + h^2\rho_{i,j}\varphi_{i,j} \end{array}\right. \\ E_k \leftarrow e \end{array}\right. \\ E \end{array}\right.$$

6)Calculating the energy values in each step of the relaxation process (fig.2)

$$N_i = 800, B = iter\_e(50,1,N_i,\rho), j = 0...N_i.$$

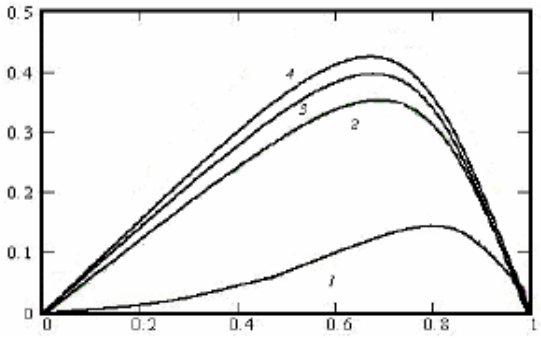

Fig. 2. The result of the calculation of energy values at each step of relaxation process.

When using this method, the following conditions must be taken into account [1]:

• choosing a good initial approximation reduces the number of necessary iterations;

• it is necessary to use the optimal value of the relaxation parameter, which can be evaluated analytically or derived empirically;

• the process may be more effective if several iterations are held for some sub-areas of the grid, in which the grid solution is known weakest, thus saving the cost of relaxation of the already relaxed part of the solution;

• to conduct calculation for the relatively coarse grid, for which the amount of computation is small, and then extrapolate the resulting solution on a fine grid and use these values as the initial approximation for subsequent iterations.

IV. SOLVING OF THE POISSON EQUATION

We shall demonstrate a relaxation method by the example of solving boundary value problem of two-dimensional Poisson's equation (2) fora square area $(0 \le x \le 1cm, 0 \le y \le 1cm)$ with known potentials at the boundaries $(u(x,0) = u(x,1) = 0)\ \ u(0,y) = u(1,y) = 0)$, assuming that there is a cell inside of the region $(0{,}4 \le x \le 0{,}6,\ \ 0{,}4 \le y \le 0{,}6)$, in which the charge is distributed uniformly with a density $\rho(\rho = 700V/cm^2)$. The algorithm containing a conductive solution to the boundary problem, is as follows:

1) setting a function that implements an iterative procedure, here $N-$ number of points in which the values of the function are calculated; w - parameter that specifies the method of relaxation; N_of_Iter- number of iterations; $\varphi-$ the matrix containing the values of the potential on the boundary and initial approximation at internal nodes; $\rho(x,y)$ the name of the function that describes the potential distribution.

$$iter2(N,\omega,N\_Iter,\varphi,\rho(x,y)) = \left|\begin{array}{l} h \leftarrow \frac{1}{N} \\ for\, i,j \in 0...N \\ \left|\begin{array}{l} y \leftarrow ih, jh \\ for\, i,j \in 0...N \\ \left|\begin{array}{l} x \leftarrow ih, jh \\ \rho_{i,j} \leftarrow \rho(x,y) \end{array}\right. \end{array}\right. \\ for\, k \in 0...N\_Iter \\ \left|\begin{array}{l} for\, j \in 1...N-1 \\ for\, i \in 1...N-1 \\ \left|\begin{array}{l} \varphi_{i,j} \leftarrow (1-\omega)\varphi_{i,j} + \frac{\omega}{4}(\varphi_{i+1,j} + \varphi_{i-1,j} + \varphi_{i,j+1} + \varphi_{i,j-1} + h^2\rho_{i,j}) \end{array}\right. \\ D_k \leftarrow \varphi \end{array}\right. \\ D \end{array}\right.$$

2)setting the grid nodes and boundary conditions

$$N = 14, i = 0...N, j = 0...N,$$
$$kx = 1...N-1, ky = 1...N-1, \mu_{i,0} = 0$$
$$\mu_{i,N} = 0, \mu_{0,j} = 0, \mu_{N,j}$$

3) Setting a function describing the distribution of the charge density in the cell

$$f(x,y) = \left|\begin{array}{l} 700 if\, (0{,}4 \le x \le 0{,}6) \cdot (0{,}4 \le y \le 0{,}6) \\ 0 otherwise. \end{array}\right.$$

4) Setting the initial approximation and the number of iterations

$$\mu_{kx,ky} = 12, N = 100, k = 0...N_i.$$

5) Calculation of the potential

$$B1_k = iter2(N,1,2,k,\mu,\rho(x,y))_k.$$

6) Mapping the equipotential level (100-th) FRAME =100 (fig. 3).

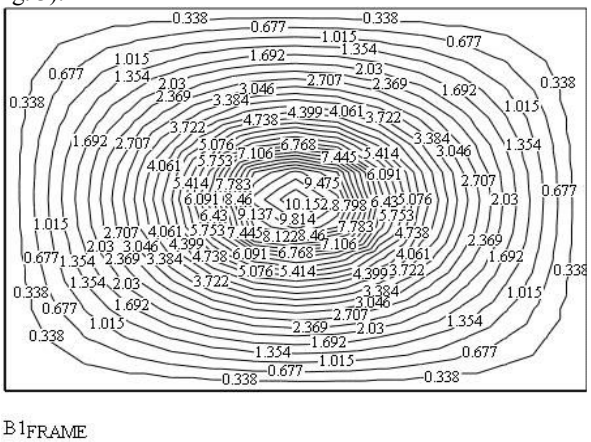

Fig. 3. Equipotential surfaces map.

In order to display the map of the equipotential surfaces after the n-th iteration, it is sufficient to assign the corresponding value of the built-in variable FRAME. However, the most visually dynamic relaxation process is noticed at consecutive considering change map equipotential surfaces at each iteration.

V. SOLUTION OF THE LAPLACE EQUATION

Let us consider the solution of the boundary problem of two-dimensional Laplace equation (1) for a square area $(0 \le x \le 1cm,\ 0 \le y \le 1cm)$ with known potentials at the boundaries

$$(\varphi(x,0) = \varphi(x,1) = 10V, \varphi(o,y) = 5, \varphi(1,y) = 5V)$$

obtained on a grid consisting of 15×15 knots (fig. 4).

$$\rho(x,y) = 0, \mu_{kx,ky} = 12,$$

$$\mu_{i,0} = 10, \mu_{i,N} = 10, \mu_{0,j} = 5, \mu_{N,j} = 5,$$

$$B1_k = iter2(N,12,k,\mu,\rho(x,y))_k,$$

$$FRAME = 100.$$

3) The task of the function describing the distribution

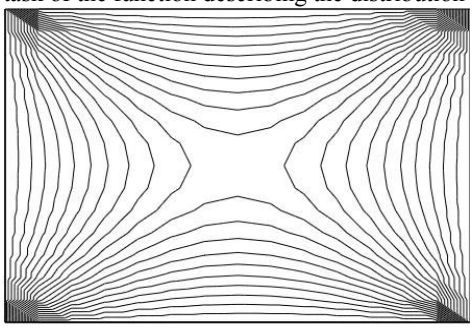

B1FRAME

Fig. 4. Maps of equipotential lines in the presence of fractures.

From fig. 4 it is seen that the lines located on the map equipotential levels are non-smooth (they have fractures in some break point). Availability of fractures, in its turn, in lines of equal potential indicates the presence of discontinuities in the derivative of the function $\vec{\nabla}\varphi(x,y)$, describing the tension of electric field. On the other hand, as we know from the theory of functions of complex variable, the function $f(x,y)$, which satisfies the Laplace equation is analytical [8-10]. Necessary and sufficient condition for analyticity of the function $f(x,y)$ is the continuity of its derivatives that are obviously not met by our obtained numerical solution. Discovered "defect" of the numerical solutions is associated with the large gird size, in which the solution of equation is sought (1). In order to eliminate it you can use two ways:

- find the numerical solution on a grid with a smaller step;
- by using a numerical solution on a grid consisting of 15×15 knots, to find values of the points which do not coincide with the grid nodes via interpolation procedure.

VI. SPLINE INTERPOLATION

Let us consider the solution of the problem on the spline interpolation function, which depends on the two variables, in Mathcad package. At that, we shall describe only a supplement to the document for solving the Laplace and Poisson equations, and therefore further we use the abovementioned introduced variables, and sequential numbering of solution steps goes on.

7) Setting vectors that contain coordinates of grid points

$$X2_i = 1/N, Y2_i = 1/N.$$

8) Creating n matrix containing the coordinates of the nodal points on diagonal of the rectangular grid Mxy = augment $(X2, Y2)$.

9) Create n of Mz matrix whose (ij) th element is the coordinate z, corresponding to the point $x = Mxy_{i,o}$ and $y = Mxy_{h,1}$:

$$M_z = B1_{N_i,}\ n = rows(M_z).$$

10) The calculation of the vector of the spline coefficients of the nodes of defined Mxy, Mz:

$$S = cspline(M_{xy}, M_z).$$

11) Setting the interpolation function

$$fit(x,y) = \text{int}erp\left[S, M_{xy}, M_z, \begin{pmatrix} x \\ y \end{pmatrix}\right].$$

12) Setting the coordinate grid in the nodes where interpolation values are computed

$$x1 = M_{xy0,0}, x2 = M_{xyn-1,0}, N_x = 6,1n, N_y = 6,1n,$$

$$y1 = M_{xy0,1} y2 = M_{xyn-1,1}, i2 = 0...N_{x-1}, j2 = 0...N_{y-1},$$

$$X_{i2} = x1 + \frac{(x2-x1)}{N_x} i2, Y_{j2} = y1 + \frac{(y2-y1)}{N_y} j2.$$

13) Calculation of the interpolation function values in the grid nodes

$$FIT_{i2,j2} = fit(X_{i2}, Y_{j2}).$$

14) The construction of equipotential lines map

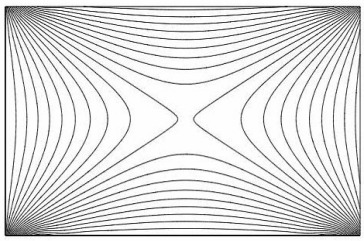

FIT

Fig. 5. Maps of equipotential lines without fractures.

Comparison of the dependences presented in fig. 4 and fig.5 shows that by using spline interpolation, it was possible to eliminate the shortcomings of the numerical solution appeared in the presence of fracture lines of equal potential. In addition, the presence of interpolating function allows you to calculate the tension and build a map of the lines of force of the electrostatic field. To do this, the algorithm needs to be complemented with the following steps.

15) Setting functions that calculates the partial derivatives at the grid points, the coordinates of which are given in the vectors x_i, y_i, and returns a vector of complex numbers in the form of:

$$Vector(X,Y,\rho(x,y)) = \left| \begin{array}{l} \Delta x \leftarrow \frac{\max(X)-\min(X)}{100} \\ \Delta y \leftarrow \frac{\max(Y)-\min(Y)}{100} \\ fori \in 0..rows(X)-1 \\ forj \in 0..rows(Y)-1 \\ Ex_{i,j} \leftarrow \frac{\rho(X_i+\Delta x,Y_j)-\rho(X_i-\Delta x,Y)}{2\Delta x} \\ Ey_{i,j} \leftarrow \frac{\rho(X_i,Y_j+\Delta y)-\rho(X_i,Y_j-\Delta y)}{2\Delta y} \\ B_{i,y} \leftarrow \frac{Ex_{i,j}+iEy_{i,j}}{\sqrt{(Ex_{i,j})^2+(Ey_{i,y})^2}} \\ B \end{array} \right.$$

16) Setting the coordinate grid, in the nodes of which the values of tension of the electric field are calculated

$$N_x = 2n, N_y = 2n, i = 0...N_{x-1}, j = 0...N_{y-1},$$

$$X1_1 = x1 + \frac{(x2-x1)}{N_x} i, Y1_j = y1 + \frac{(y2-y1)}{N_y} j \cdot$$

17) Calculation of a vector comprising a complex number of unit length

$$B2 = Vector(X1, Y1, fit).$$

18) Visualization of tension of the electrostatic field (fig.6).

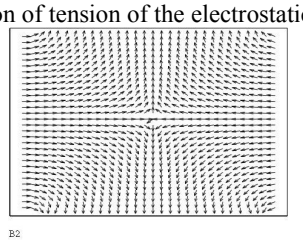

Fig. 6. Visualization of tension of the electrostatic field

CONCLUSIONS

1. Developed a new algorithm to allow creating an animated clip of the relaxation process of numerical solution of the Laplace equation to the exact solution, using the spline interpolation map of the power equipotential lines on each step of iteration.
2. Created an animated clip to allow following the tension evolution of the electric field in the process of relaxation.
3. Justified the necessity of the use of the optimum value of the relaxation parameter, which can be evaluated analytically or obtained empirically.
4. Demonstrated that the process can be more effective if you spend a few iterations on certain grid subdomains in which the grid solution is known weakest, thus saving the cost of relaxation of the already relaxed parts of the solutions.
5. Conducted calculation on the relatively coarse grid, for which the amount of computation is small, and the resulting solution is then extrapolated to a fine grid and these values were use as the initial approach for subsequent iterations.

REFERENCES

[1] Islamov, I.J. Transaction of Azerbaijan Academy of Sciences, Series of Physical-mathematical and Technical sciences, Physics and Astronomy, XXIV №2 (2004) 48-57.

[2] Islamov, I.J. Transaction of Azerbaijan Academy of Sciences, Series of Physical-mathematical and Technical sciences, Physics and Astronomy, XXIII №2 (2003) 205-214.

[3] Ismibayli, E.G., Islamov, I.J., Gaziyev, Y.G. Calculation Of The Electromagnetic Field Of The Microwave Of Devices With Use Of Method FDTD And Integral Kirchhoff. International Journal of Engineering Innovation and Research (IJEIR), Volume 5, Issue 1, (2016) 103-106.

[4] Ismibayli, E.G., Islamov, I.J., Gaziyev, Y.G. Modeling Of Electromagnetic Fields Of Microwave Devices On The Basis Of Matlab Program. International Journal of Innovative Science, Engineering and Technology (IJISET), Volume 3, Issue 2, (2016) 61-63.

[5] Ismibayli, E.G., Islamov, I.J., Gaziyev, Y.G. An Optimal Control Of An Electromagnetic Field In High-Powered Microwave Devices. International Journal of Trend in Research and Development (IJTRD), Volume 3(1), (2016) 246-249.

[6] Ismibayli, E.G., Islamov, I.J., Gaziyev, Y.G. Modeling of Anisotropic Rectangular Waveguide Partially Embedded in an Anisotropic Substrate. Journal of Multidisciplinary Engineering Science and Technology (JMEST). Vol. 2, Issue 2, (2015) 153-157.

[7] De Moerloose Jan, Dawson Trevor W., Stuchly Maria A. Application of the finite difference time domain algorithm to quasi - static field analysis. Radio Sci. -32, №2 (1997) 329-341.

[8] Iomota V., Alotto P. Magnetic field computation in media with hysteresis. Rev. roum. sci. techn. Ser. Electrotechn. et energ. -41, №3 (1996) 291-296.

[9] Koshiba M., Okada M., Suzuki M. Numerical analysis of two - dimensional piezoelectric waveguides for surface acoustic waves by finite-element method. "Electron. Lett.", №17 (1981) 609-611.

[10] Miller Edmund K., Burke Gerald J. Lowfrequency computational electromagnetics for antenna analysis. Proc. IEEE. - 80, N1 (1992) 24-43